Pergamon

Journal of Structural Geology, Vol. 16, No. 11, pp. 1555 to 1573, 1994

0191-8141/94 $07.00+0.00

0191-8141(94)00056-5

Transpression and transtension within different structural levels in the central Aegean region

KONSTANTINOS BORONKAY and THEODOR DOUTSOS

Department of Geology, University of Patras, 26110, Greece

(*Received* 23 *September* 1993; *accepted in revised form* 21 *April* 1994)

Abstract—In the central Aegean region, shortening structures within the Miocene molasse are known since long ago. Nevertheless recently, most authors have recognized extensional structures within Middle to Upper Miocene granitoids, proposing a *Basin and Range* type model for the Late Cenozoic evolution of the area. To resolve this problem, structural mapping and mesoscopic analysis of 900 faults sampled from 12 islands have been carried out.

Late orogenic uplift of the central Aegean region is the result of a continuous convergence and indentation of the Pelagonian plate by the Apulian plate, that took place throughout the Miocene. Formation of core-complexes can be associated with: (a) large oblique-upthrusts, (b) steeply dipping strike-slip faults, and (c) low-angle normal faults. The latter are produced by low, multidirectional extension, which has affected small crustal regions as adjacent areas underwent transpression. In the late stages of collision the overthickened crust began to collapse due to transtension which was replaced by extension caused by the roll-back of the Hellenic subduction zone in the Lower Pliocene time. This extensional regime has lasted until the present day.

INTRODUCTION

THE nature of late orogenic uplift of collisional mountain belts represents one of the major topics in tectonics today. There is strong debate as to the relative merits of two kinematic models, that of *syn-compressional uplift* and continuous underplating (Hsü 1991) and that of *extensional metamorphic complexes* (Davis 1983, Lister & Davis 1989). Attempts to combine the two schools of thought have been made by Coney & Harms (1984) and Platt (1986) who proposed that compression and extension took place synchronously or successively at different structural levels. However during recent years, the classic way of thinking, which may have overestimated movements taking place perpendicular to the strike of the belts, has gradually been replaced by new mobilistic ideas, proposing that tectonic escape and extrusion processes have contributed strongly to the late orogenic evolution of collisional mountain belts (Tapponnier & Molnar 1977, Ratschbacher *et al.* 1991, Vauchez & Nicolas 1991).

The central Aegean islands, comprising an Alpine blueschist belt which was intruded by late kinematic granites and covered by molassic sequences (Fig. 1) (Jacobshagen *et al.* 1978), is an area in which most of the above mentioned hypotheses have been applied (Fig. 2). Most studies have been supported by data collected mainly in granites often on only one island. We carried out structural mapping and mesoscopic analysis of 900 faults collected from granites as well as from the molassic cover in 12 islands to arrive at an overall picture of crustal movements.

TECTONIC SETTING

The central Aegean region is part of the Attic-Cycladic massif, which together with the Pelagonian massif belongs to the central Hellenides (Fig. 1) (Jacobshagen *et al.* 1978). It is composed of a stacked sequence of nappes mainly established during the Alpine orogeny in the Early Eocene (Marinos & Petraschek 1956, Dürr *et al.* 1978). However relics of a Hercynian basement have been reported on many islands (Kreuzer *et al.* 1978, Henjes-Kunst & Kreuzer 1982, Andriessen *et al.* 1987). Although the tectonostratigraphy is well known on individual islands the correlation between the islands is difficult (Okrusch & Bröker 1990). Despite new work carried out in the area, we adopt the nappe classification of Dürr *et al.* (1978) with some modification and we distinguish four main units, from bottom to top (Fig. 1).

(1) *The basal unit* represents an anchimetamorphic carbonate platform of Late Triassic to Late Cretaceous neritic limestones conformably overlain by a Paleocene flysch; e.g. on Amorgos, Tinos, Thyra and Samos (Tataris 1964, Melidonis 1980, Avigad & Garfunkel 1989). This platform has been generally considered as equivalent to parts of the Apulian platform lying further west (Fig. 1). Alternatively, it may represent remnants of a microcontinent lying between the Apulian and Eurasian plates, analogous to the Ossa and Olympos platforms, further north in the Hellenic peninsula (Jones & Robertson 1991, Doutsos *et al.* 1993).

(2) *The Chora unit* of Bonneau (1984) consists of orthogneisses, granitoids and paragneisses of Hercynian age (Ios, Sikinos, Naxos, Syros).

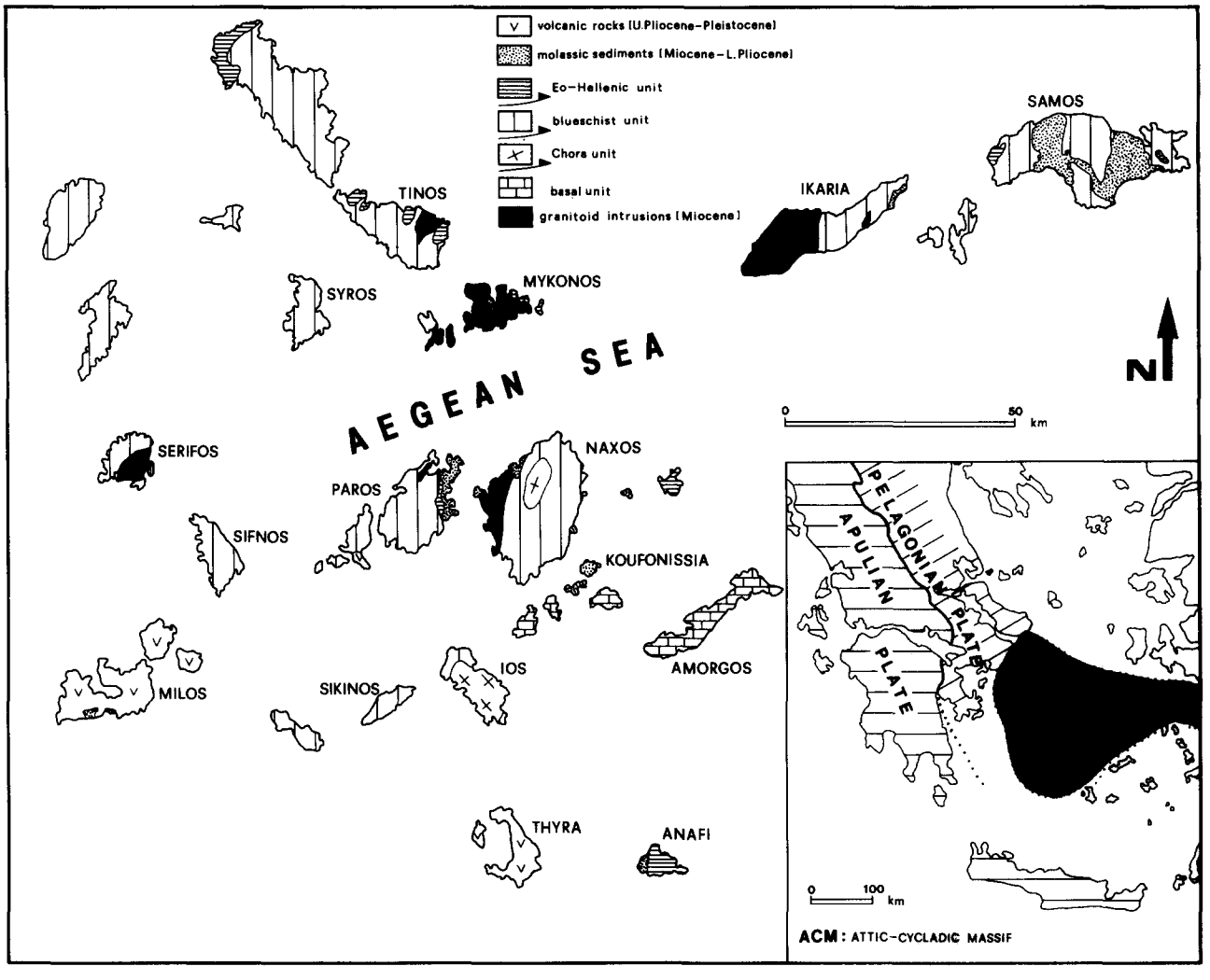

Fig. 1. Simplified geological map of the Attic-Cycladic massif (I.G.M.E. 1983), showing main tectonostratigraphic units (modified from Dürr *et al.* 1978). Inset shows Apulian and Pelagonian plates and the site of Attic-Cycladic massif (ACM).

(3) *The blueschist unit* was originally a Mesozoic continental margin consisting of neritic carbonates, psammitic to pelitic sedimentary rocks, and basic and acid volcanics. In the Early Eocene (40–45 Ma) this margin was subducted and metamorphosed under temperatures of 450–500°C and at minimum pressures of 14 kbar (Dixon 1976, Altherr *et al.* 1982). Later, in the Late Oligocene (25 Ma) this metamorphism was followed by a Barrovian-type metamorphism (450–480°C and 4–7 kbar) culminating in the formation of thermal domes as in Naxos and Sifnos islands (Jansen & Schuiling 1976, Okrusch *et al.* 1978, Andriessen 1978, Schliestedt *et al.* 1987). Maximum metamorphic conditions of this phase (670–700°C and 6–7 ± 2 kbar) took place in the core of the thermal domes, where migmatites were formed (Wijbrans & McDougall 1988, Buick & Holland 1989).

(4) *The Eohellenic unit*, sensu Jacobshagen *et al.* (1978), consists of two sub-units: an ophiolitic sub-unit on top covered by Upper Cretaceous limestones and a melange sub-unit of Permo-triassic limestones, with greenschists and intrusive rocks at the base (Dixon & Ridley 1987). Metamorphism of this unit is low-grade and is dated to be Late Cretaceous (70 Ma, Reinecke *et al.* 1982, Patzak 1988).

During the Miocene, all tectonic units were intruded by I- and S-type granitoids (Marakis 1970, Altherr *et al.* 1982, Henjes-Kunst *et al.* 1988). These rocks were crystallized at high levels in the crust at depths of 5–10 km as deduced from metamorphic assemblages in the country rocks (Altherr *et al.* 1982, Buick 1991a,b). Somewhat later, extensive andesitic volcanism took place at the Earth's surface (Fytikas *et al.* 1984, Pe-Piper & Piper 1989).

Throughout the Miocene, at the same time as the emplacement of the granites, molassic sediments accumulated. In many islands the Lower Miocene lies unconformably above the Eohellenic unit (i.e. Paros Island, Dermitzakis & Papanikolaou 1980). In other islands, the Lower Miocene is missing and the Upper Miocene transgressed the lower structural units (Samos Island, Theodoropoulos 1979). However, Jansen (1973) and Roesler (1978) recognized tectonic contacts between molasse and the basement in the island of Naxos. Later, a low-angle tectonic contact between the molasse and the underlying granites in Mykonos is dated to be of Late Miocene age, supporting the existence of a gravity slide (Dürr & Altherr 1979, Dermitzakis & Papanikolaou 1980, Böger 1983).

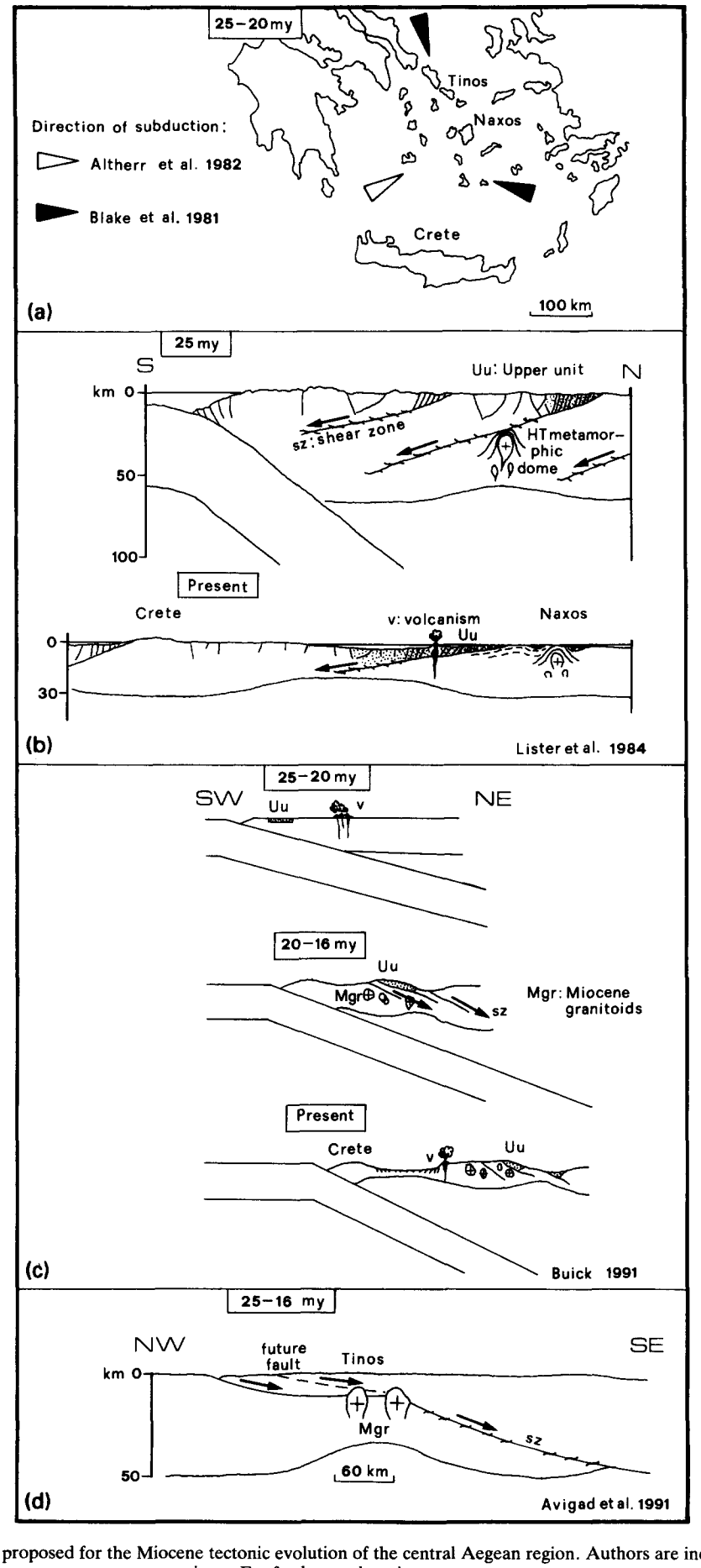

Fig 2. Models proposed for the Miocene tectonic evolution of the central Aegean region. Authors are indicated in each inset. For further explanations, see text.

Several different models have been published in recent years to explain late orogenic uplift in the Aegean region.

(1) Uplift was caused by compression (Angelier 1977a,b) and continuous underplating of the Apulian platform below the Eurasian plate (Fig. 2a) (Jansen 1973, Altherr *et al.* 1982).

(2) Emplacement and uplift of the granites took place along a NE-trending, right-lateral transform fault which separated two subduction segments named Alpidic and Cycladic, respectively (Fig. 2a) (Blake *et al.* 1981).

(3) Uplift was induced by a *Basin and Range* type extensional mechanism in which metamorphic core complexes were exhumed in the footwall of a southerly dipping low-angle shear zone of normal character (Fig. 2b) (Lister *et al.* 1984, Ridley 1984). Later this model was modified by Buick (1991b) (Fig. 2c), who suggested that subduction of the Hellenic trench (LePichon & Angelier 1979) led to extension by means of north dipping, low-angle normal faults in the Aegean back arc basin.

(4) Uplift and extension result from compression in other parts of the Hellenides (Fig. 2d) (Avigad & Garfunkel 1989, 1991). In this interpretation, the contact between the Eohellenic and the blueschist unit is a low-angle normal fault, along which the Eohellenic unit was transported for more than 200 km. The direction of extension implied in this model is at right angles to the northeast–southwest convergence of the Hellenides during the Neogene.

From the above models, it is apparent that extensional tectonics has played an increasingly important role in recent interpretations of uplift in the Aegean area. This area has become a classic area for studies of large magnitude extension of continental crust. Our studies will emphasize the role of Miocene compression and wrenching which took place synchronously with the extension in other parts of the region. This leads us to propose a transpressional model for the uplift in the central Aegean area.

STRUCTURES IN THE MOLASSIC COVER

Structures within the molassic cover are interpreted as formed in the course of two events: an older transpressional event and a younger transtensional event. Superposition of transtensional structures onto transpressional structures varies considerably from island to island, and therefore we distinguish islands with dominant transpressional structures and islands where transtensional structures prevail. However, some islands have only been affected by the transtensional event.

Islands with dominant transpressional structures

Samos. On Samos Island, two Neogene basins filled with terrigeneous sediments are separated by a basement high of blueschists: the Mytilini basin to the east and the Karlovassi basin to the west (Fig. 3a).

(1) The Mytilini basin contains Upper Astracian/Valecian lacustrine limestones along its western margin and Turolian/Pliocene fluviolacustrine conglomerates, tuffs and limestones along its eastern margin (map of Fig. 3a) (Meissner 1976, Weidmann *et al.* 1984). The basin floor is tilted westward so that the strata thickness is asymmetric, being thickest (about 800 m) along the western margin of the basin (Fig. 3a: F–F′). This margin is marked by an arcuate fault called Mavradzei Fault forming a structural relief of more than 2 km. Kinematic parameters change gradually along the strike of the fault. The northern branch of the fault is a NW-trending overthrust showing northeast directed displacements (Fig. 3a: D–D′). It served as a conduit for magma which was concordantly intruded into the unconsolidated sediments in the footwall of the fault. The latter was internally deformed by NE-trending, very tight to close chevron folds. (Fig. 3a, plot 5). The central branch of the Mavradzei Fault shows a right-lateral oblique-thrust slip. It is segmented and rotated clockwise into a north–south position by four NE-trending transcurrent faults which show a right-lateral displacement (Fig. 3a, map). To the east, the Neogene basin forms a major flexure (Fig. 3a: E–E′) carrying folds and thrusts trending NNE or ENE, parallel to the central branch of the fault and the transcurrent faults respectively (Fig. 3a, plot 5). Folds are kink-like in shape, open and verge mainly eastwards. However, conjugate and W-verging folds have also been observed. Toward the east, folds and thrusts become wider spaced whereas strata are slightly rotated, suggesting that deformation decreases eastward. Restoration of the cross-section D–D′ of Fig. 3(a) yields a horizontal shortening of about 1 km. In addition, taking into account that this shortening was achieved during deposition of the Mytilini formation (i.e. between 11 and 8 Ma, Van Couvering & Miller 1971) we calculate a convergence rate for this branch of the fault to be in the order of 3 mm y^{-1}. The southern branch of the Mavradzei Fault dips very steeply and shows a strike-slip character. Strata in the footwall of the fault are very slightly rotated, whereas internal deformation dies out only a few decametres from the fault (Fig. 3a: F–F′).

Summarizing, the Mavradzei Fault is a transpressional fault with a northern frontal thrust which gradually becomes a strike-slip fault southwards. Thus a strain partitioning along the Mavradzei Fault is identified. The Mytilini basin in the footwall of this fault has mainly resulted from a combination of right-lateral wrenching and overthrusting.

In order to determine the stress tensor responsible for the kinematic character of this transpressional fault population we carried out computer calculations (Etchecopar *et al.* 1981, Oncken 1988). Results define a horizontal σ_1 (maximum compressive stress) trending E–W, and σ_2 (intermediate compressive stress) and σ_3 (minimum compressive stress) dipping moderately to the south and north respectively (Fig. 3a, plot 4).

However, the upper strata in the basin show a different evolution. The upper two thirds of the clastic series

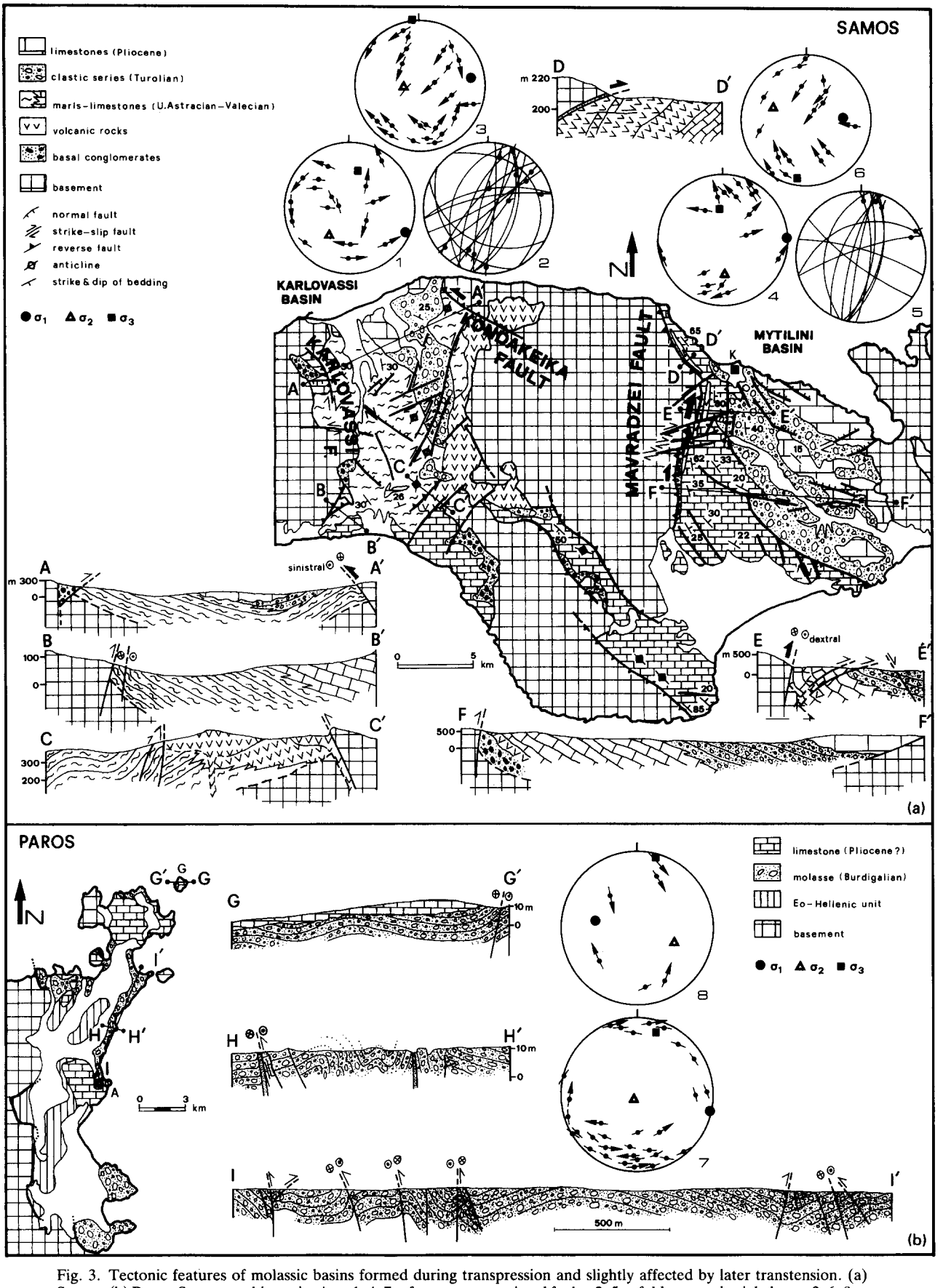

Fig. 3. Tectonic features of molassic basins formed during transpression and slightly affected by later transtension. (a) Samos. (b) Paros. Stereographic projections 1, 4, 7 refer to transpressional faults, 2, 5 to fold axes and axial planes, 3, 6, 8 to transtensional faults. Stereographic projections 1, 2, 3 and 4, 5, 6 include tectonic data collected from Karlovassi and Mytilini basins, respectively. K—Kokkari, G—Glaronisi islet, A—Ambelas.

as well as the overlying limestone formation, deposited since 7 Ma until present, are deformed only by oblique-normal faults. They comprise moderately dipping, E–W to WNW oblique-normal faults and steeply dipping NE transfer faults (Fig. 3a, plot 6). Near Kokkari, two WNW-trending faults, running parallel to the coast have been mapped (Fig. 3a). They dip toward the north at angles of 60° and show left-lateral oblique-normal slip. These faults caused an antithetic rotation of the downthrown blocks (estimated at 30–40°, Fig. 3a) and display a maximum vertical displacement of 200 m. Syn-sedimentary tectonism is indicated by rapid changes of the sedimentary facies and the presence of large wedge-shaped sedimentary prisms in the hanging wall of the faults. As these faults control changes in the morphology and the drainage pattern they may also have a neotectonic origin. Analysis of slip data along the faults indicates that the faults were formed in the frame of a transtensional regime. The calculated σ_3 axis trends N–S, whereas σ_2 and σ_1 axes plunge WNW and ESE, respectively, (Fig. 3a, plot 6).

(2) The Karlovassi basin contains a clastic sequence, which is thought to be stratigraphically equivalent to the Neogene sediments deposited in the Mytilini basin (Theodoropoulos 1979). Like the Mytilini basin, the Karlovassi basin also shows a dominantly transpressional origin. The northern part of the basin is downflexed by two NW-trending thrusts, namely the Karlovassi Fault and the Kondakeika Fault, which border the western and eastern margins of the basin, respectively (Fig. 3a, map). To the south the Karlovassi Fault curves gradually into a NNE position. In the same direction NNE-trending right-lateral faults and ENE-trending left-lateral transcurrent faults become denser. Both fault sets are associated with similar trending folds and served as conduits for magma and hydrothermal fluids. Fault breccias within faults are typically silicified, apparently by fluids and heat associated with andesitic dyke emplacement. Frictional heating in this shear zone could facilitate fluid migration and enhance partial melting as is observed in other transpressional regimes (Strong & Hanmer 1981). Analysis of fault slip data indicates a similar stress tensor to that calculated for the Mytilini basin (Fig. 3a, plot 1).

Transtensional faults have affected only the northern part of the basin where the Lower Pliocene limestones are deposited. Analysis of slip data along these faults indicates a similar stress distribution to the upper parts of the Mytilini basin (Fig. 3a, plots 3 and 6).

Paros. A NNE-trending molassic basin lies unconformably above an ophiolitic basement in eastern Paros. It consists of Burdigalian conglomerates, sands, sandy clays and clays (Dermitzakis & Papanikolaou 1980) underlain by Upper Miocene silicified calcareous sandstones and conglomerates (Böger 1983). Angelier (1977b) interpreted the structural evolution of the basin to be the result of E-verging folding and thrusting. However, most of the faults described as thrusts show a considerable component of horizontal movement and thus have a transpressional character (Fig. 3b: I–I′). Folds are confined to narrow zones near the faults. On the coastline at Ambelas, a NNE-trending fault is associated with highly rotated beds near the faults, 2.5 m thick cataclasite, and folds whose amplitudes are up to 10 m (Fig. 3b: H–H′). However, at a distance of 80 m from the fault, folds die out and beds become gradually horizontal. Oblique striae and splaying patterns of en échelon mesoscopic faults, as well as the offsets of individual segments of the faults, suggest left-lateral, oblique-thrust character. Further north, on the Glaronisi islet (Fig. 3b: G–G′) growth folds with depocentres in synclines and condensed sequences over anticlines indicate syn-sedimentary tectonism.

In several places another set of NW-trending right-lateral and ENE-trending left-lateral, oblique-thrusts were formed. Cross-cutting relationships between the principal NNE- and WNW-trending faults indicate that both sets of faults were contemporaneous. The computed stress tensor for this population of transpressional faults is characterized by compression in an east-southeast direction, where σ_1 bisects the acute angle of NW- and ENE-trending faults (Fig. 3b, plot 7).

Although the molassic basin in Paros is a typical transpressional basin, some WNW–trending oblique normal faults, which dislocate and cross-cut older transpressional structures, indicate that the late stages of the basin evolution were influenced by a transtensional stress regime (Fig. 3b, plot 8).

Naxos. Molassic sediments, cropping out as erosional remnants above the granodiorites in the western and northern parts of Naxos, show similar structural evolution to the molassic basin in Paros (Fig. 4c, plots 6, 7).

Islands with dominant transtensional structures

In the western part of Anafi Island a clastic sequence of Upper Miocene conglomerates, sands and red clays crops out (Böger 1983), separated from the pre-Neogene basement by a steeply dipping NNE-trending fault (Fig. 4a). Kinematic indicators along small faults, such as sigmoidal flexures on the scale of 1–10 m, mesoscopic folds and slickensides, suggest right-lateral, oblique-thrust movements. In the footwall of the marginal fault three other NNE-trending faults with forward and backthrust components form a 300 m wide zone of transpressional structures. Further west the tectonic pattern changes to transtensional. A 700 m wide asymmetric horst is bounded by N–S to NW-trending oblique-normal faults. Moderate- to low-angle dipping faults imply high magnitude of extension (Fig. 4a: A–A′).

In some islands transpressional structures are very weakly developed. In Mykonos Island, as Angelier (1977a) has first recorded, barite dykes intruded along NW-trending left-lateral, oblique-thrust faults (Fig. 4b: C–C′). In only a few cases these faults are accompanied by NW-trending mesoscopic folds. In Milos Island, strike-slip faults are very rare whereas folds are found

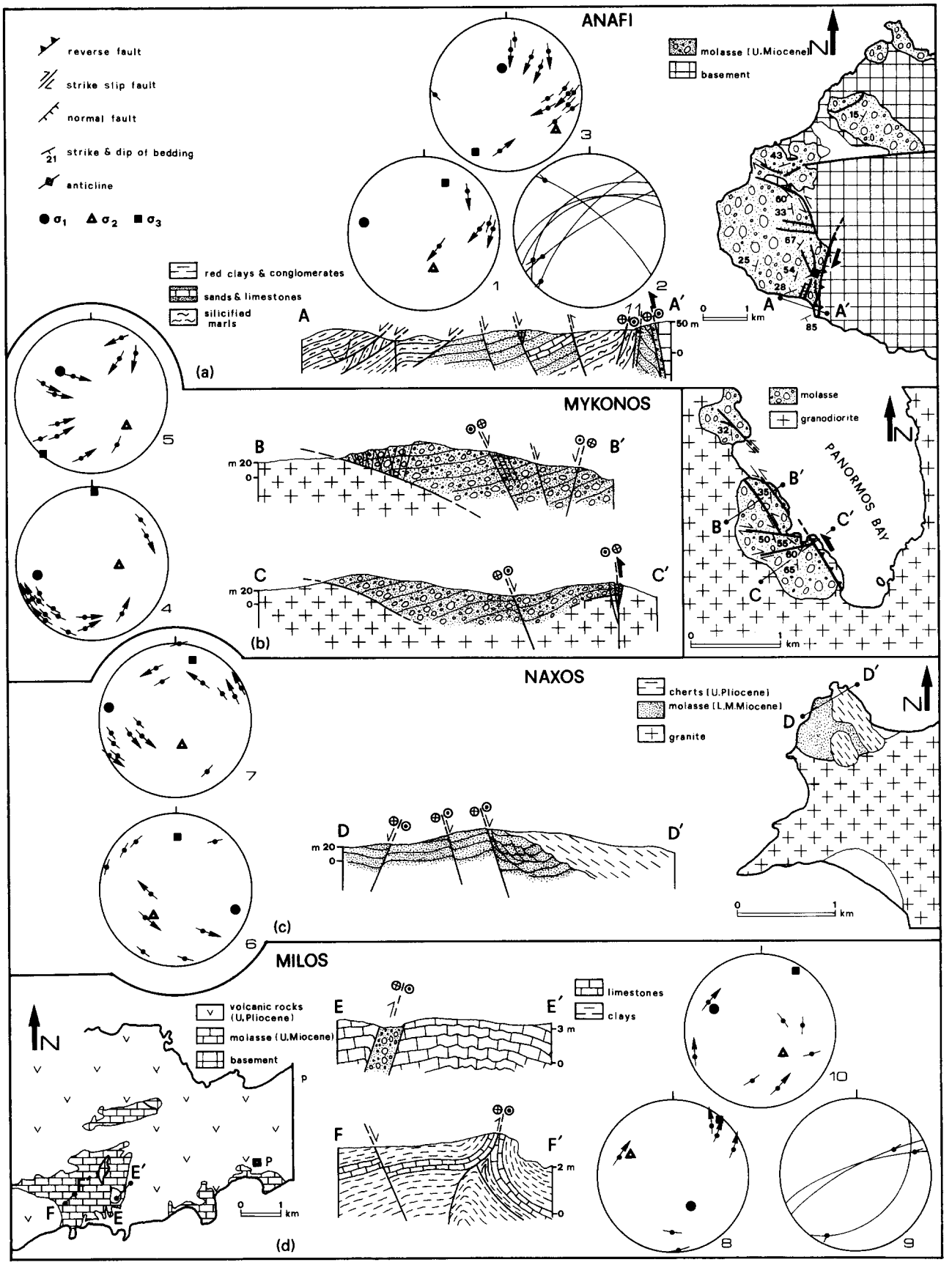

Fig. 4. Tectonic features of molassic basins with minor transpressional and dominant transtensional structures. (a) Anafi. (b) Mykonos. (c) Naxos. (d) Milos. Stereographic projections 1, 4, 6, 8 refer to transpressional faults, 2, 9 to fold axes and axial planes and 3, 5, 7, 10 to transtensional faults (tectonic symbols refer to all illustrations). P—Provatas.

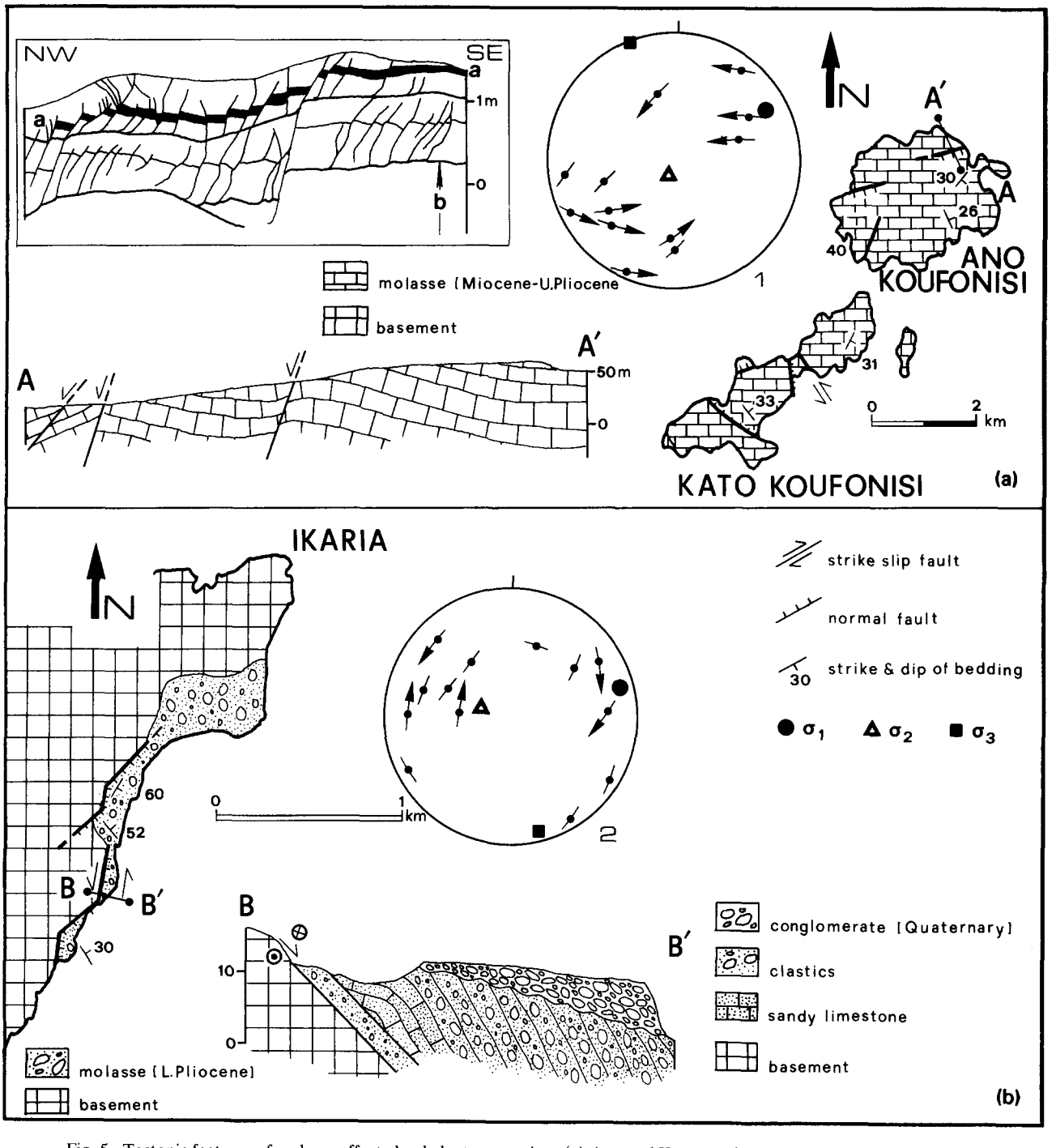

Fig 5. Tectonic features of molasse affected only by transtension. (a) Ano and Kato Koufonisi. (b) Ikaria. Stereographic projections 1, 2 refer to transtensional faults with striations. Cross-section of inset in (a) consists of a sedimentary package of psammitic limestones with clay intercalations (**a** and **b**). Location of the cross-section is at the northwestern coastline of Kato Koufonisi (tectonic symbols refer to both illustrations).

only in two outcrops in a roadcut west of Provatas (Fig. 4d: E–E′, F–F′).

Islands affected only by transtension

The Ano and Kato Koufonisi Islands provide excellent exposures of Upper Miocene limestone and clastic deposits (Böger 1983) that show how oblique-normal faults develop at depth. Most of the E–W to WNW-trending oblique-normal faults, cross-cutting vertical cliffs, are sigmoidal in shape, becoming asymptotic to the dominant bedding-parallel slip downwards. Common characteristics of listric normal faults, such as roll-over anticlines with highly rotated layering, and smaller synthetic and antithetic faults (c.f. Doutsos and Poulimenos 1992) are observed here (Fig. 5a inset). However, in some outcrops, planar faults bound domino-like blocks. Dip separation on the faults ranges from a few meters to 200 m but on most faults the separation is less than 50 m.

Calculations of percentage extension, using the dip of fault surface and bedding (Wernicke & Burchfiel 1982)

compared with restoration of the cross-section, have shown a mean magnitude of 24% (inset cross-section of Fig. 5a).

A small occurrence of Lower Pliocene clastic deposits (Ktenas 1969) in the eastern part of Ikaria Island is deformed only by strike-slip transtensional faults (Fig. 5b, plot 2).

STRUCTURES WITHIN THE GRANITES

Pluton emplacement in the central Aegean islands is largely controlled by upper crustal tectonism as indicated by the interaction of progressive crystallization with one to three tectonic events. Separation of the various tectonic events has been made possible by the direct field observation of superposition and cross-cutting relationships of interfering structures, commonly occurring in a single granitic outcrop. Therefore we start our structural description from granites with the simplest structural evolution.

Ios

On Ios, about ten small granitic plutons intruded into Hercynian orthogneiss (Van der Maar & Jansen 1983). We focus on the structural characteristics of the well-exposed Psathi granite. This granite is well differentiated with a weak magmatic foliation observed in some places. Pegmatitic and aplitic dykes are absent. Slight deformation within the granitic body is represented by low-angle, NW-dipping shear surfaces (Fig. 6, 6; Fig. 7b). Fine-grained retrograde mineral assemblages (sericite + chlorite + quartz) on these surfaces indicate deformation under low greenschist facies conditions. Extensional cleavage associated with these shear surfaces shows top to the north-northwest shear movements. Also, slickensides found in thin cataclasites (up to 1.5 m thick, Fig. 7b: B–B′) associated with the metamorphic aureole in the northwestern border of the granite, show oblique-normal movements. At some places all these structures have been displaced by a set of NE-trending steeply dipping normal faults.

From the above we conclude that the Psathi granite is syn-tectonic in relation to a regional tensional phase which took place under brittle–ductile transition conditions.

Paros

Several small granitic plutons intruded in the northwestern part of Paros Island during the Late Miocene (11 Ma, Altherr *et al.* 1982). We concentrate our study on the well exposed northernmost granitic body, the Naoussa granite, 3 km west of Naoussa. This pluton is a concordant one, laccolithic in shape (Fig. 7a: block diagram, A–A′) which has domed up the paragneiss series into which it intruded. The paragneiss series of the roof was bent up and flattened strongly. This is indicated by ductile normal faults, an extensional cleavage, and boudinage in the pegmatitic and aplitic sills, emplaced parallel to the gneissic foliation. The margins of the pluton display a low-angle southwest dipping solid state foliation formed at temperatures of 550–650°C, as is indicated by feldspar ductility (Paterson *et al.* 1989). A downdip stretching lineation (Fig. 6, 8 plot DT), on the foliation is defined by elongate feldspar, biotite and quartz aggregates. About 100 m from the edge of the pluton the foliation becomes less pervasive, whereas the centre of the pluton remains undeformed. ESE- to NE-trending pegmatitic and aplitic dykes (Fig. 6, 8 plot A) generally cross-cut the foliation although some dykes predate shear movements. All sense of shear indicators such as sigmoidal porphyroblasts, *S–C* relations, feldspar imbrication and displacement of dykes are consistent with ESE-directed extensional shear.

From the above we conclude that the Naoussa granite is syn-tectonic in relation to a small extension under ductile conditions.

Mykonos

Upper Miocene granites crop out over much of Mykonos Island (Altherr *et al.* 1982). In the field, the most prominent and widespread structure is a low-angle, NE-dipping, solid state foliation which displays a downdip stretching lineation (Fig. 8a, B–B′; Fig. 6, 3 plot DT). Kinematic indicators reveal northeast directed extensional motion (Faure & Bonneau 1988, Faure *et al.* 1991, Lee & Lister 1992). Mylonite zones up to 3 m thick are spaced 100–300 m apart (Fig. 8a, B–B′) and contain synthetic and antithetic shear bands indicating strong flattening. In Panormos Bay these mylonite zones are displaced by NW-trending steeply dipping faults or fault zones. These zones are commonly up to 1 km thick and are several km in length cross-cutting the whole island (Fig. 8a, A–A′). Low temperature mineral assemblages, such as chlorite + epidote found within cataclasites of this fault zone, indicate that these structures were formed under brittle–ductile transition conditions. Subhorizontal striations on fault surfaces within the fault zone indicate extensive strike-slip movements as also recorded within the molassic cover on top of the granitic body. The kinematic character of the faults is the result of two successive events, a former transpression and a later transtension (Fig. 6, 3 plots BDTP, BTT).

We conclude that the granite in Mykonos was emplaced during ductile extension, later modified by transpression and transtension under brittle–ductile and brittle conditions, respectively.

Serifos

On Serifos, a Late Miocene (10–9 Ma) granodioritic intrusion caused intensive contact metamorphism with skarn formation (Salemink 1985, Altherr *et al.* 1982). The northeastern border of the pluton is a complex zone of granodiorite with variable composition (granodiorite to more differentiated granite), textures (fine to coarse grained), and basement interleaves (Fig. 8c, F–F′). Basement interleaves are ductilely deformed exhibiting

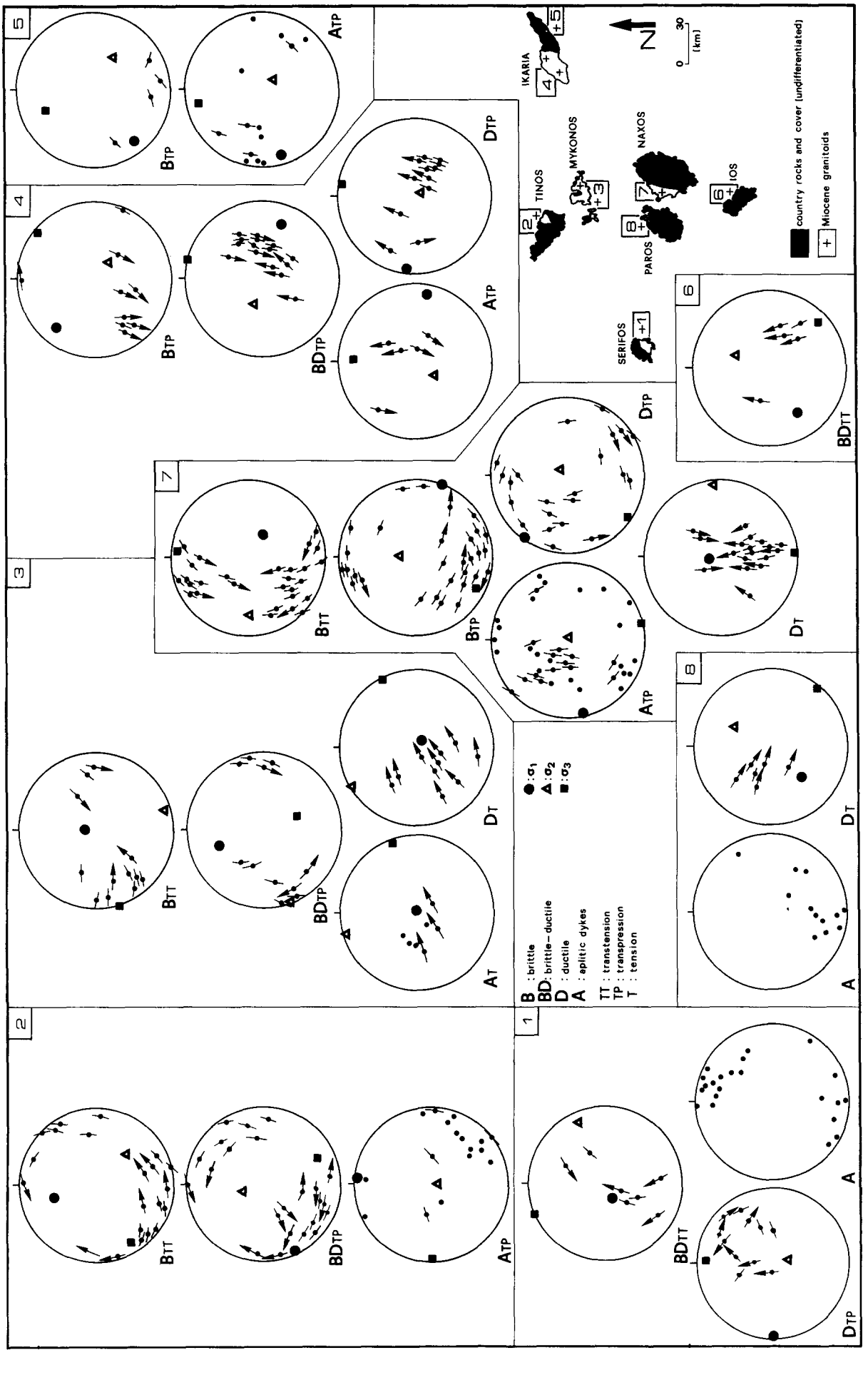

Fig. 6. Stereographic projections of structural data and directions of the corresponding principal stresses of granitoid intrusions. Ductile structures include mylonites and solid-state foliation; brittle–ductile transition structures include pseudotachylytes, fault zones with retrograde mineral assemblages; and brittle structures include cataclasites and brecciated fault zones. Numbers on top of each column refer to the simplified inset map.

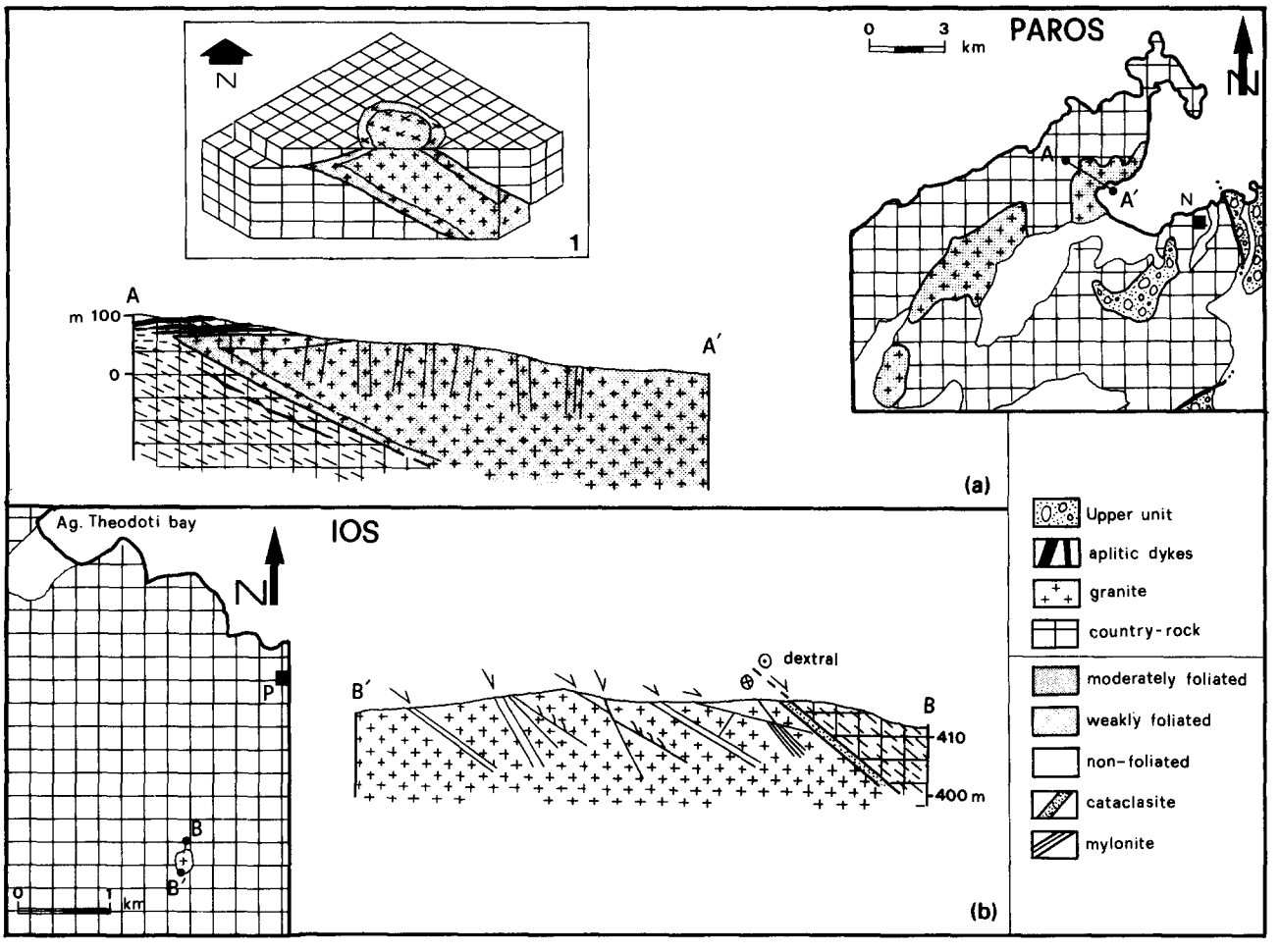

Fig. 7. Maps and cross-sections of granitoids which intruded during extension. (a) Paros. (b) Ios. Block diagram (inset 1) refers to the intrusion pattern of the Naoussa granite. N—Naoussa, P—Psathi (for further explanations see text).

mylonites with a prominent NW–SE striking planar foliation. Mylonites are also observed in granodiorite, showing greenschist facies mineral parageneses (epidote + actinolite) (Salemink 1985). They are NW-trending and are confined to the border of the granodioritic interleaves. The thickest (0.5 m) mylonite zone borders the main intrusive body and is parallel to a 50 m thick hydrothermal alteration zone (Fig. 8c, F–F'). Shear bands in these mylonites show left-lateral, oblique-thrust movements that resulted from a transpressive regime where σ_1 is horizontal and trends E–W (Fig. 6, 1 plot DTP). Country-rocks were intruded by several aplitic dykes up to 8 m thick.

Toward the centre of the granitic body ductile deformation diminished rapidly and is represented only by closely spaced (1–10 m) shear (*C*) planes. WNW- to ENE-trending, steeply dipping aplitic dykes (Fig. 6, 1 plot A) are cross-cut by these surfaces which display slickensides showing predominantly oblique-normal movements (Fig. 6, 1 plot BDTT). As in the granite of Ios, steeply dipping normal faults offset all previous structures.

We conclude that the Serifos granite is syn-tectonic with a regional transpressional event which took place under brittle–ductile transition conditions during consolidation of magma.

Tinos

In the northeastern part of Tinos Island, granitic rocks intruded during the Middle Miocene (15–14 Ma) into blueschists and amphibolites and caused intensive contact metamorphism (Melidonis 1980, Altherr *et al.* 1982). The pluton is ovoid-shaped with a northeast major axis trending parallel to the structural trend of the wall rocks (Fig. 8b). A weak alignment of K-feldspar megacrysts and clots of biotite and/or hornblende may reflect a foliation before full crystallization. The northwestern border of the granitic body is characterized by a 1 km thick highly strained zone (map of Fig. 8b). It consists of thick (up to 5 m) WNW-trending mylonites and superimposed pseudotachylytes (Fig. 6, 2 plot BDTP). Offset of dykes, small-scale intrafolial folds and *S–C* foliations indicate top to the southwest sense of shear along the NE-dipping stretching lineation. To the north, along a spectacular outcrop near the coast, the granite interleaves with blueschist and intrudes along syn-magmatic ductile faults (Fig. 8b: E–E'). This contact acted as the ascent conduit for pegmatitic and aplitic magmas (Fig. 6, 2 plot ATP). To the east, in the Livadas Bay (Fig. 8b: C–C'), ductile deformation is absent and the granite is separated by the ophiolitic basement along a NW-trending, steeply dipping fault. This fault is associated

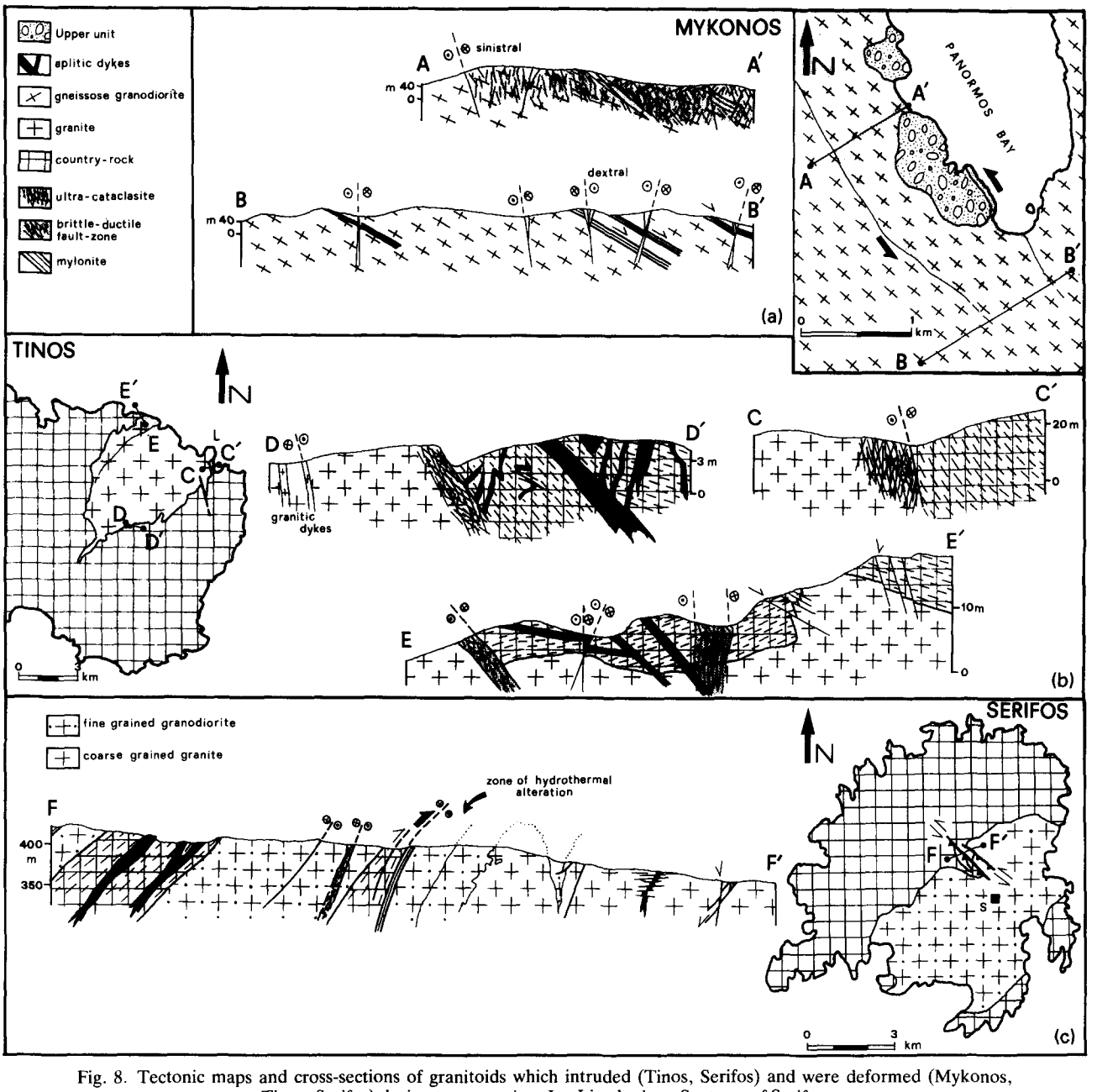

Fig. 8. Tectonic maps and cross-sections of granitoids which intruded (Tinos, Serifos) and were deformed (Mykonos, Tinos, Serifos) during transpression. L—Livadas bay, S—town of Serifos.

with 10 m thick cataclasites and displays a left-lateral kinematic character. The southern border of the pluton shows similar structural characteristics (Fig. 8b: D–D') where pegmatites and aplites intruded concordantly and/or discordantly both into the granitic body and the wall rocks.

Faults form a conjugate system of east-northeast right-lateral and northwest left-lateral strike-slip faults. These faults are classified in two populations based on cross-cutting relationships, different conditions during the formation of structures, and fault planes with two striations. Stress analysis reveals that these faults were formed in the course of two successive phases, an older transpressional under ductile and brittle–ductile conditions and a younger transtensional under brittle conditions (Fig. 6, 2 plot BDTP, BTT).

We conclude that the Tinos granite is a discordant granite showing syn-tectonic emplacement in relation to a transpressional regime acting under ductile and later modified to brittle–ductile transition conditions.

Ikaria

The western half of Ikaria Island is occupied by a large granitic body which crystallized in the Miocene (Altherr *et al.* 1982). Its eastern contact with the Mesozoic country rocks is complex and consists of two segments (Fig. 9b, map): (1) a southern intrusive contact, and (2) a northern tectonic contact, the Ikaria Fault, associated with mylonites (Ktenas 1969), along which the granite was overthrust eastward (Ktenas 1969) or northward (Papanikolaou *et al.* 1991) onto the Mesozoic basement.

The granite in the western part of the island can be divided into two sub-units: (1) a lower undeformed subunit of porphyritic granodiorite forming an intrusive contact with the basement, and (2) an upper, intensely

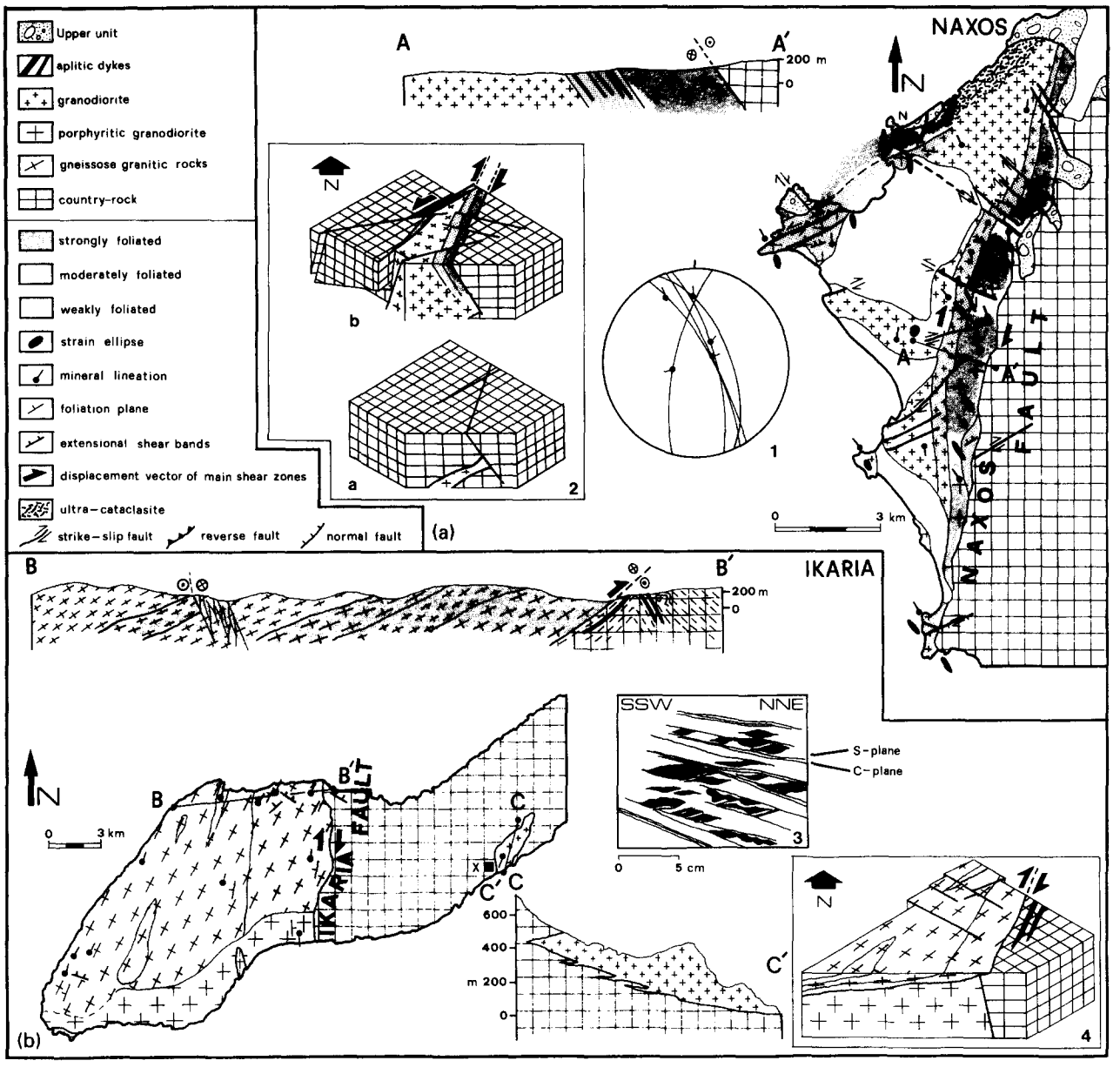

Fig. 9. Tectonic pattern of Naxos (a) and Ikaria (b) granitoids which comprise a complex, successive tectonic history. 1: Stereoplot of fold axes and axial planes adjacent to Naxos Fault. 2: Schematic evolutionary block diagram of the Naxos granitoid. (a) Intrusion of magma along a ENE-trending low-angle shear zone (13 Ma) and (b) magma ascent along the Naxos Fault. 3: Illustration of a hand-specimen showing the relationship of *S–C* planes indicating top to the NNE sense of shear. 4: Schematic block diagram showing the present structure of Ikaria granitoid. Normalized *XY*-principal-plane strain ellipses are obtained from deformed enclaves (for methods see Ramsay & Huber 1983, Hutton 1988). N—town of Naxos, X—Xylosyrtis.

deformed subunit of gneissose granitic rocks adjacent to the Ikaria Fault (Fig. 9b: block diagram). The last subunit is internally deformed by a pervasive low-angle, NW-dipping solid state foliation carrying a pronounced NNE-trending stretching lineation (Fig. 9b and Fig. 6, 4 plot DTP). High strain is concentrated along three mappable mylonite zones up to 1.5 km thick (Fig. 9b). Within these mylonite zones, folds, shear zones of oblique–reverse character, *S–C* surfaces (Fig. 9b, inset 3) and minor normal faults show top to the north-northeast sense of shear. All structures show ductile deformation which occurred within biotite zone mineral parageneses, characterized by essentially complete recrystallization of the igneous assemblage. To the east of the tectonic contact, wall rocks are strongly deformed within a 1.2 km wide zone by chevron and kink folds with axial planes trending parallel to the fault (Fig. 9b: B–B′).

In the early stages of the ductile deformation WNW- to NNW-dipping aplitic dykes intruded both the granitic body and the narrow, strongly deformed zone in the wall rock. Cataclastic texture at the edge of late quartz veins, quartz vein apophyses, and the occurrence of pseudotachylytes suggest that deformation continued into brittle–ductile transition conditions. All aplitic dykes and quartz veins have undergone strike-slip movements during the intrusion (Fig. 6, 4 plot ATP, BDTP). Finally, a conjugate system of NW- and ENE-trending strike-slip faults was formed (Fig. 6, 4 plot BTP; Fig. 9b: B–B′).

The most likely kinematic interpretation is that the Ikaria Fault is a right-lateral, oblique-thrust, along

which the upper sub-unit of gneissose granites detached from the lower undeformed sub-unit and moved northwards. Such major décollement zones occur at 15 km depth and are common features in regions affected by strike-slip faults (for review see Sylvester 1988). This interpretation demonstrates that the granite was still being emplaced while the Ikaria Fault was active. Subhorizontal slickensides on quartz veins and pseudotachylytes suggest that last increments of movements on the Ikaria Fault outlived the magmatic stage.

Another, small laccolithic intrusion near Xylosyrtis village (Fig. 9b: C–C′, Ktenas 1969) was deformed under brittle conditions only (Fig. 6, 5 plot BTP).

Naxos

In the western part of Naxos Island, granodiorite intruded during the Middle Miocene (13–11 Ma) into the blueschist unit causing contact metamorphism (Jansen 1973, Altherr *et al.* 1982). In the western part of the pluton, a flat-lying magmatic foliation is commonly cross-cut by a low-angle NNW-dipping solid state foliation (Fig. 9a). NNW-dipping stretching lineation on the solid state foliation (Fig. 6, 7 plot DT), extensional shear band geometries and asymmetric micafish indicate top to the north-northwest movement.

Toward the eastern margin of the granodiorite all these structures are cross-cut by a younger mylonitic foliation, which is defined by a sequence of small-scale layers up to 0.1 mm in width and composed of chlorite, sericite, quartz and minor actinolite crystals. It is approximately parallel to the borders of the pluton (Fig. 9a) and contains decimetric to microscopic intrafolial folds. Strain ratio estimates on ellipses defined by enclaves within the granodiorite (for methods see Ramsay & Huber 1983, Hutton 1988) reveal a positive gradient and an increasing ratio of simple shear to pure shear toward the eastern margin of the pluton. Mylonites are common throughout a 1.5 km wide zone and are grouped into two NNE-trending subzones (Fig. 9a): an eastern one with strain ratios of 6–12 consisting of ultramylonites and mylonites, and a western one with strain ratios of 2–6 consisting of proto-mylonites (Fig. 6, 7 plot DTP) intruded by pegmatitic and aplitic dykes (Fig. 6, 7 plot ATP).

Intrafolial folds within the mylonites of the eastern sub-zone (stereoplot of Fig. 9a) commonly cluster close to a NNE-trending stretching lineation. Toward the pluton border, the angle between the fold axial traces and the metamorphic contact decreases whereas fold axes show steep plunge (70–80°). Adjacent to the metamorphic aureole in the country rock, fold axes plunge at high angles and the foliation displays a younger NNE-plunging stretching lineation. Such strain partitioning into components parallel and normal to the faults is reported from many strike-slip terrains in the world (Fitch 1972, Zoback *et al.* 1987, Reutter *et al.* 1991, Cobbold *et al.* 1991). All the above kinematic characteristics lead us to interpret the granodiorite border with the metamorphic rocks of central Naxos as a right-lateral ductile shear zone (Naxos Fault) with a small thrust component.

Country rocks of the metamorphic aureole have also been affected by these movements (F_2 and F_3 folds of Buick 1991a,b). Further east in the hanging wall of the Naxos Fault, regional deformation and metamorphism in lower amphibolite to greenschist facies continues until 7 Ma (Andriessen *et al.* 1979), which is simultaneous with cooling of the granodiorites. In this area, doming and partial melting took place in the core of mappable NNE-trending upright folds (Jansen 1973, post-peak M_{2B} structures of Buick 1991a,b). Therefore we infer that ductile shearing along the Naxos Fault was synchronous with doming and horizontal shortening in its hanging wall rocks.

Abundant quartz veins and pegmatite dykes are confined to the moderately deformed sub-unit of the mylonitic granodiorites adjacent to the Naxos Fault (Fig. 9a: A–A′). They are up to 1 m thick, up to 70 m in length, and are closely spaced (1–1.5 m). Most dykes dip moderately E–ESE and display slickensides indicating strike-slip movements (Fig. 6, 7 plot ATP). From the above we interpret that the Naxos Fault acted as a 'fault valve' allowing a large fluid circulation system to evolve.

The amount of displacement along the Naxos Fault is unknown. However a minimum displacement along the fault can be estimated from inferred shear strains. If we take a mean thickness of the mylonite zone of about 1.5 km and a mean strain ratio of 8, a minimum displacement of 12 km results. As cooling ages of undeformed granodiorites are given at 11.1 ± 0.7 Ma and pseudotachylytes are 9.9 ± 0.4 Ma old, we infer a time interval of 1.2 ± 1.1 for the formation of mylonites. Thus minimum displacement rates may be in the order of 0.6 cm y^{-1}.

Furthermore, a conjugate system of ENE- and NW-trending faults was formed within the granodiorite. Splay cracks along the fault planes are often filled with minerals including epidote, chlorite and quartz, a characteristic mineral assemblage of the chlorite zone metamorphic facies. Faults are associated with dilation breccias with angular fragments, attrition breccias and gouge layers, up to 5 m thick. Although the majority of these faults are pure strike-slip faults, some of these display a small reverse component. Computed stress distribution responsible for the kinematic character of these faults is σ_1: ESE, σ_3: SSW and σ_2 nearly vertical (Fig. 6, 7 plot BTP).

In the late stages of deformation ENE- and WNW-trending oblique-normal faults were formed within the granodiorite, as a result of a transtensional mechanism. During the transition from transpression to transtension, the σ_3 axis remained constant whereas the σ_1 gradually rotated from an initial horizontal to a final moderately dipping position (Fig. 6, 7 plot BTT). These younger faults are often reactivated older strike-slip faults, as the latter sometimes exhibit two generations of striations.

We conclude that structural evolution of the granodiorite in Naxos includes three tectonic events: (a) an extensional event, during which granodiorite was

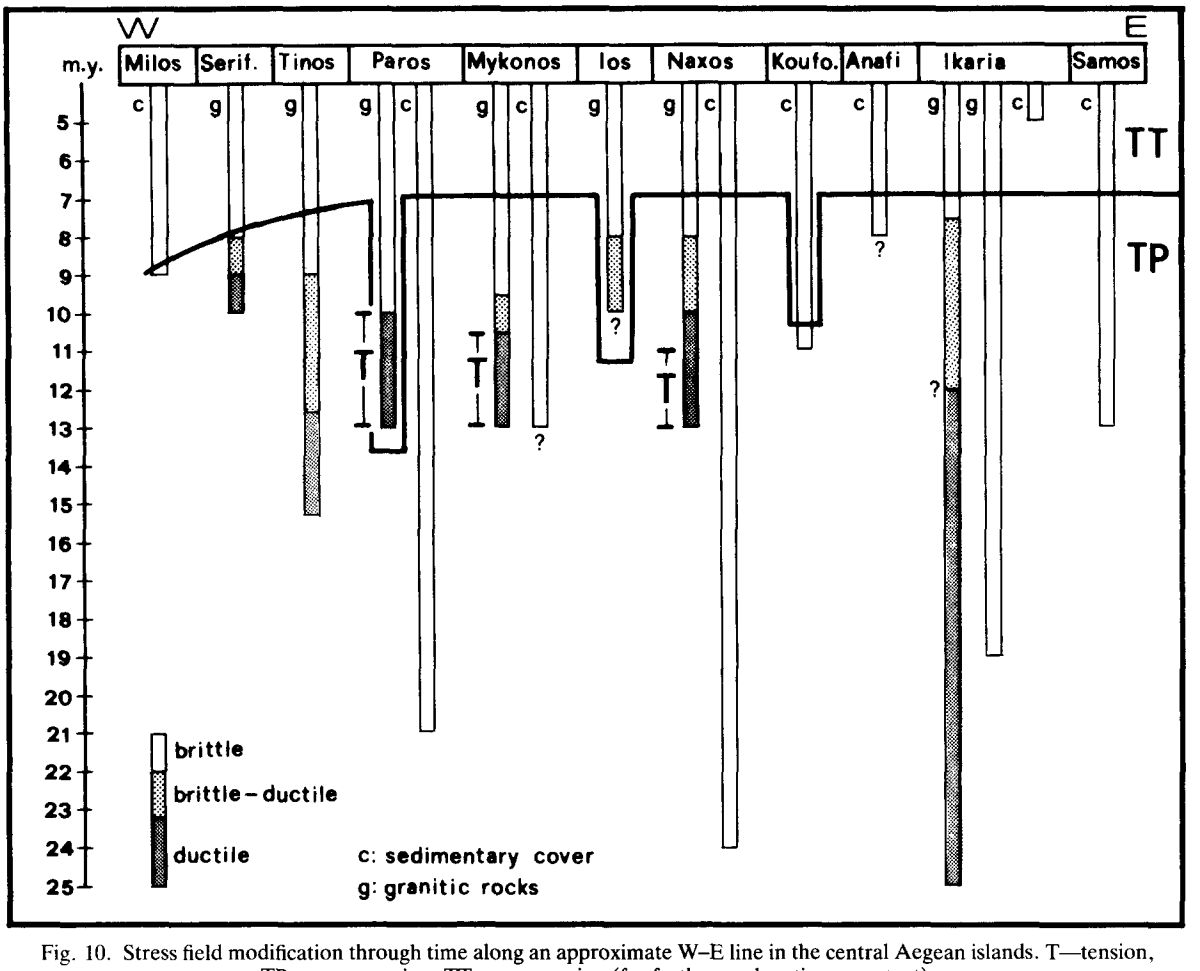

Fig. 10. Stress field modification through time along an approximate W–E line in the central Aegean islands. T—tension, TP—transpression, TT—transtension (for further explanations, see text).

emplaced, (b) a transpressional event, which took place under ductile to semi-ductile conditions producing shear zones along which magma rose up, and (c) a transtensional event which took place under brittle conditions.

SUMMARY OF STRUCTURAL CHARACTERISTICS

Deformation in the sedimentary cover

The sedimentary cover was deformed by transpression and transtension in two successive stages (Fig. 10).

(1) Transpression controlled the evolution of molassic basins in the Samos, Paros and Naxos Islands throughout Miocene and produced large pop-up structures i.e. Samos Island (Fig. 11). Islands with Late Miocene deposits such as Samos, Mykonos, Anafi and Milos have been moderately or strongly affected by transpression. The computed σ_1 stress axis varies considerably between ENE and ESE, and caused NNE-trending right-lateral faults and NW-trending left-lateral faults. Both fault sets grade in places into oblique-thrusts and are often associated with en échelon folds and thrusts. They served as conduits for the intrusion of volcanic rocks (e.g. Samos Island) or mineral dykes (e.g. Mykonos Island). The NNE-trending set of faults is preferentially developed than the NW-trending set (Fig. 11). On all islands transpression terminated at 7 Ma (Fig. 10).

(2) Transtension began in the Koufonisia and Milos Islands in the Late Miocene while transpression continued in other islands (Figs. 10 and 11). σ_1 rotated gradually from an horizontal to a moderately dipping position suggesting that the transpressive regime was gradually replaced by the transtensional one. The computed σ_3 stress axis varies between SSE and SSW and caused ENE- and WNW-trending oblique-normal faults, commonly with a listric geometry. As rotation of σ_1 continued through time, it became vertical in Lower Pliocene and the whole crust extended in tension.

Deformation within the granites

The lower parts of the upper crust have also been affected by two successive stages resulting from transpression and transtension as it is indicated by the emplacement and ascent mechanism of the granites and their internal structures.

(1) Transpressional structures comprise a conjugate system of NNE-trending right-lateral faults and NW-trending left-lateral faults. (a) The first set of faults is preferentially developed in the eastern part of the study area (Fig. 11). In Naxos, a NNE-trending strike slip fault (Naxos Fault) separates a transpressional core complex

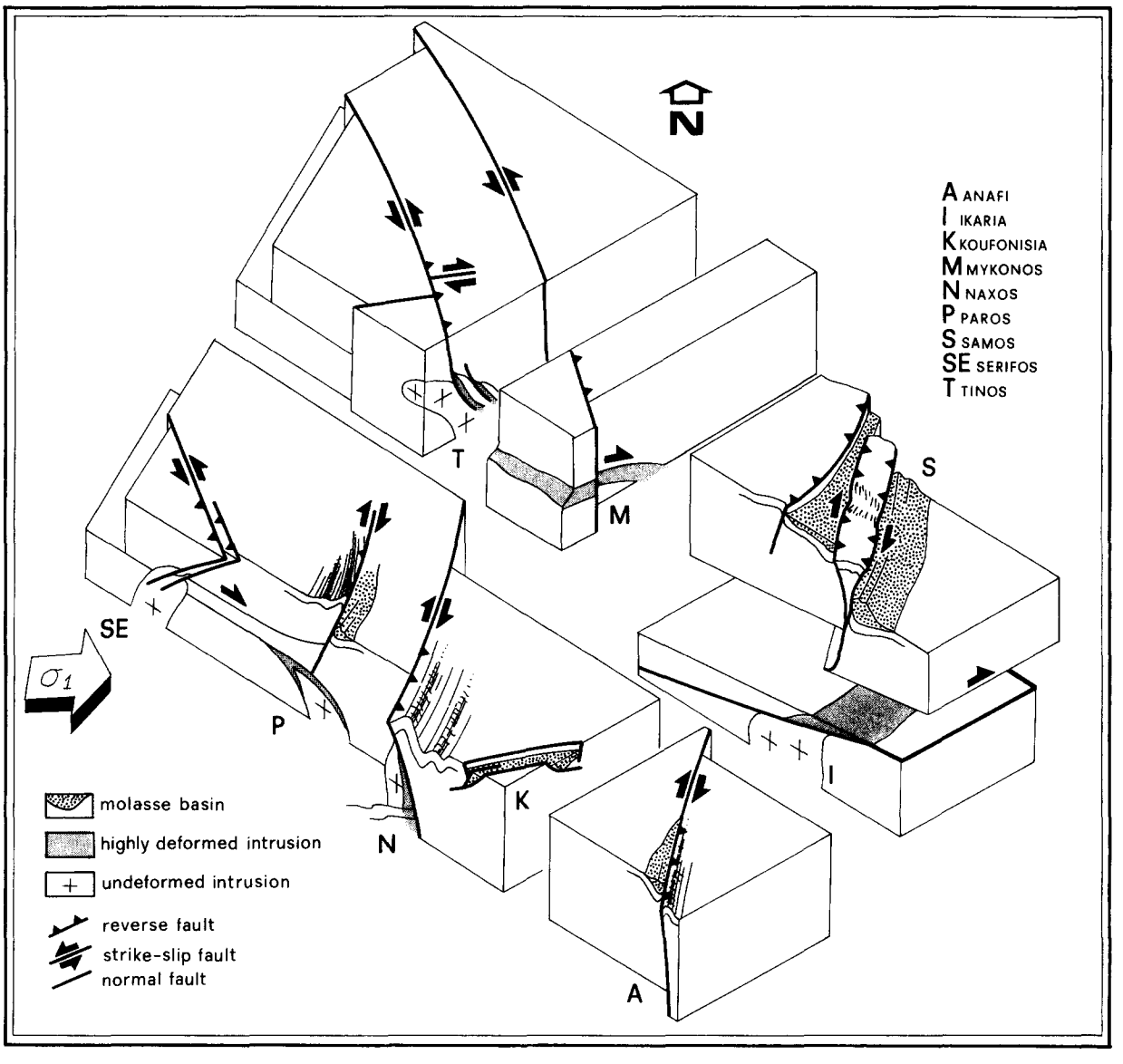

Fig. 11. Interpretative three-dimensional model for the upper crust of the central Aegean region during the Miocene. Transpression leads to the formation of pop-up structures (Samos) and transpressional core-complexes (Naxos, Ikaria). Granitic magmas rise up along crustal scale transpressional faults (Tinos, Serifos, Naxos); these faults die out within flat-lying detachment shear zones at depth (15 km) where magma intrudes syn-tectonically (Ikaria). At the same time, extension facilitates the intrusion of granitoids (Mykonos, Paros, Naxos). Transtension synchronous to transpression on the surface produces small grabens (Koufonisia).

on its hangingwall from a strongly foliated granodiorite on its footwall. In Ikaria, a NNE-trending oblique-thrust (Ikaria Fault) separates strongly deformed from undeformed granites. (b) The second set of faults occurred mainly in the western part of the study area (Fig. 11). In Serifos a magmatic, NE-trending contact is strongly modified by NW-trending oblique-thrusts associated with thin mylonites. In Tinos along a NW-trending oblique-thrust the granite was overthrust above the blueschist unit and in Mykonos granites were cross-cut by NW-trending left-lateral faults.

(2) Transtensional structures comprise ENE- to WNW-trending *S–C* shear zones and similar trending oblique-normal faults formed during the late stages of structural evolution of the granites. In Ios, the emplacement of a small granite took place exclusively under transtension.

Extensional core-complexes. Some granites in the central Aegean region are syn-tectonic in relation to an extensional event acting in a time interval between Lower and Upper Miocene. Several authors considered this extension as a *discrete extensional phase* which has strongly affected the whole Aegean crust from Upper Oligocene until today (Lister *et al.* 1984, Buick 1991b, Avigad & Garfunkel 1991). Our structural data do not support this statement for the following reasons. (1) Extension within the granites was too weak. Thus we observe essentially undeformed to weakly deformed granites showing widely spaced thin mylonites (i.e. Mykonos Island). In Naxos Island older mylonites, related to extension, are much thinner than younger ones formed in a transpressive regime. Also, in places where the molassic cover is extended, the extensional ratio never exceeds 30% (i.e. Koufonisia Islands). (2)

Extension is multidirectional, changing from island to island. (3) Extension within the granites took place simultaneously with strike-slip faulting and shortening (Fig. 10).

Our study reveals that extension during the Miocene is weak and multidirectional, affecting small crustal regions, while adjacent areas undergo transpression.

TECTONIC SYNTHESIS

The main Alpine orogeny in the central Aegean, including the nappe formation and the two metamorphic events, is thought to be a result of the closure of the Mesozoic Pindos ocean during collision of the Apulian and Pelagonian plates (Fig. 1) (Bonneau 1984). We consider here only the post Oligocene, late orogenic evolution of the area to establish an uplift model (Fig. 11).

Uplift caused by transpression

Our study reveals that at several places in the central Aegean region, convergence of the Apulian and Pelagonian plates continued throughout the Miocene. A conjugate system of NNE- and NW-trending pure strike-slip faults associated with en échelon folds and oblique-thrusts was formed during this late stage of collision. The dominance of NNE-trending strike-slip faults in the area indicates that the convergence of the Apulian and Pelagonian plates was oblique.

Transpressive structures controlled the evolution of the molassic basins as well as the ascent, siting and emplacement of the granites. These structures led to convergent thickening and uplift of the Aegean crust, as it is observed in many transpressive shear zones (Harding & Lowell 1979, Sanderson & Marchini 1984, Burgman 1991). The results of transpression would be an overthickened root which would be pushed down into the mantle provoking partial melting of the crust (Leake 1990). Moreover, from a study of the Ibero-Armorican arc and the British Caledonides, Hutton & Reavy (1992) concluded that steeply dipping shear zones may not only control the emplacement mechanisms of plutons but they may also cause the genesis of the granites themselves. If this is the case in the central Aegean region, then extensional structures observed in the early stages of the structural evolution of some granites (Naxos, Mykonos Islands) were formed in a pull-apart setting near large strike-slip shear zones. Such a strike-slip zone may be an ENE-trending transcurrent fault separating two orogenic domains of different structural evolution in the Aegean area (Fig. 2a) (Blake *et al.* 1981). Along this zone the majority of the granites in our study area crop out.

Another way to explain early extensional structures in the central Aegean region is convergence of irregular margins, as is the case in other mountain belts (Burke & Sengör 1986). We can assume that in small areas, incomplete collision led to extensional collapse, whereas in adjacent areas plate convergence continued. This is the case further north, in the Mesohellenic trough, where at the front of the Apulian indentors plate convergence continued until the Upper Miocene, whereas locally, collapse began earlier in the Upper Oligocene (Doutsos *et al.* 1994). However, mapping of such indentors in the Aegean area requires seismic profiles and a better understanding of the surface geology.

Post-orogenic collapse

As mentioned above collapse of the overthickened crust is diachronous (Fig. 10) and produced ENE- to WNW-trending oblique-normal faults. The σ_1 axis rotated gradually from a horizontal position, becoming vertical in Lower Pliocene. Since Lower Pliocene the whole crust in the Aegean area underwent extension as a back arc basin, induced by the rollback of the Hellenic subduction zone (LePichon & Angelier 1979).

Acknowledgements—We are grateful to O. Oncken for providing us with his latest version of a computer program determining stress tensor from fault striation analysis, and for helpful discussions on the computed results. We also thank two anonymous reviewers for valuable comments.

REFERENCES

Altherr, R., Kreutzer, H., Wendt, I., Lenz, H., Wagner, G. A., Keller, J., Harre, W. & Höhndorf, A. 1982. A late Oligocene/Early Miocene high temperature belt in the Attic-Cycladic crystalline complex (SE Pelagonian, Greece). *Geol. Jb.* **E23**, 97–164.

Andriessen, P. A. M. 1978. Isotopic age relations within the polymetamorphic complex of the island of Naxos (Cyclades, Greece). *Verh. ZWO-Laboratorium voor Isotopen-Geologie*, Amsterdam **3**, 1–71.

Andriessen, P. A. M., Banga, G. & Hebeda, E. H. 1987. Isotopic age study of pre-Alpine rocks in the basal units on Naxos, Sikinos and Ios, Greek Cyclades. *Geologie Mijnb.* **66**, 3–14.

Andriessen, P. A. M., Boelrijk, N. A. I. M., Hebeda, E. H., Priem, H. N. A., Verdurmen, E. A. T. & Verschure, R. H. 1979. Dating the events of metamorphism and granitic magmatism in the Alpine Orogen at Naxos (Cyclades, Greece). *Contr. Miner. Petrol.* **69**, 215–225.

Angelier, J. 1977a. Sur l'évolution tectonique depuis le miocène supérieure d'une arc insulaire mediterranéen: l'arc égéen. *Rev. Geogr. Phys. Geol. Dyn.* **19**(3), 271–294.

Angelier, J. 1977b. Essai sur la néotectonique et les dernières stades tarditectoniques de l'arc égéen et d'Egée méridionale. *Bull. Soc. geol. Fr.* **1110**, 651–662.

Avigad, D. & Garfunkel, Z. 1989. Low angle faults above and below a blueschist belt-Tinos Island, Cyclades Greece. *Terra Nova* **1**, 182–187.

Avigad, D. & Garfunkel, Z. 1991. Uplift and exhumation of high-pressure metamorphic terrains: the example of the Cycladic blueschist belt (Aegean Sea). *Tectonophysics* **188**, 357–372.

Blake, M. C., Bonneau, M., Kienast, J. R., Lepvrier, C., Maluski, H. & Papanikolaou, D. 1981. A Geological reconnaissance of the Cycladic blueschist belt, Greece. *Bull. geol. Soc. Am.* **92**, 247–254.

Böger, H. 1983. Stratigraphische und tektonische Verknüpfungen kontinentaler Sedimente des Neogens im Ägäis-Raum. *Geol. Rdsch.* **72**, 771–814.

Bonneau, M. 1984. Correlation of the Hellenides nappes in the south-east Aegean and their tectonic reconstruction. In: *The Geological Evolution of the Eastern Mediterranean* (edited by Dixon, J. E. & Robertson, A. H. F.). *Spec. Publs. geol. Soc. Lond.* **17**, 517–527.

Buick, I. S. 1991a. Mylonitic fabric development on Naxos, Greece. *J. Struct. Geol.* **13**, 643–656.

Buick, I. S. 1991b. the late Alpine evolution of an extensional shear zone, Naxos, Greece. *J. geol. Soc. Lond.* **148**, 93–103.

Buick, I. S. & Holland, T. J. B. 1989. The *P–T–t* path associated with

crustal extension, Naxos, Cyclades, Greece. In: *Evolution of Metamorphic belts* (edited by Daly, J. S., Cliff, R. A. & Yardley, B. W. D.). *Spec. Publs. geol. Soc. Lond.* **43**, 365–370.

Burgmann, R. 1991. Transpression along the southern San Andreas fault, Ourmia Hill, California. *Tectonics* **10**, 1152–1163.

Burke, K. & Sengör, A. M. C. 1986. Tectonic escape in the evolution of the continental crust. In: *Reflection Seismology: The Continental Crust* (edited by Barazangi, M. & Brown L. D.). *Am. Geophys. Un. Geodynamic Series* **14**, 41–53.

Cobbold, P. R., Gapais, D. & Rossello E. 1991. Partitioning of transpressive motions within a sigmoidal foldbelt: the Variscan Sierras Australes, Argentina. *J. Struct. Geol.* **13**, 743–758.

Coney, P. J. & Harms, T. A. 1984. Cordilleran metamorphic core complexes: Cenozoic extensional relics of Mesozoic compression. *Geology* **12**, 550–554.

Davies, G. H. 1983. Shear zone model for the origin of metamorphic core complexes. *Geology* **11**, 342–347.

Dermitzakis, M. & Papanikolaou, D. 1980. The molasse of Paros Island, Aegean Sea. *Ann. Naturhist. Mus. Wien* **83**, 59–71.

Dixon, J. E. 1976. Glaucophane schists of Syros (abstract). *Bull. geol. Soc. Fr.* **8**, 280.

Dixon, J. E. & Ridley, J. R. 1987. Syros. In: *Chemical Transport in Metasomatic Processes* (edited by Helgeson, H. C.). Reidel Publishing Company, 489–501.

Doutsos, T. & Poulimenos, G. 1992. Geometry and kinematics of active faults and their seismotectonic significance in the western Corinth-Patras rift (Greece). *J. Struct. Geol.* **14**, 689–699.

Doutsos, T., Pe-Piper, G., Boronkay, K. & Koukouvelas, I. 1993. Kinematics of the Central Hellenides. *Tectonics* **12**, 936–953.

Doutsos, T., Koukouvelas, I., Zelilidis, A. & Kontopoulos, N. 1994. Intracontinental wedging and postorogenic collapse in the Mesohellenic Trough. *Geol. Rdsch.* **83**, 257–275.

Dürr, S. & Altherr, R. 1979. Existence de klippes d'une nappe composite Néogène dans l'île de Mykonos/Cyclades, Grèce. *Rapp. Comm. Int. Mer Mediter.* **25/26**, 33–34.

Dürr, S., Altherr, R., Keller, J., Okrusch, M. & Seidel, E. 1978. The median Aegean crystalline belt: stratigraphy, structure, metamorphism, magmatism. In: *Alps, Apennines, Hellenides* (edited by Cloos, H., Roeder, D. & Schmidt, K.). Schweizerbart, Stuttgart, 455–476.

Etchecopar, A., Vasseur, G. & Daignieres, M. 1981. An inverse problem in microtectonics for the determination of the stress tensors from fault striation analysis. *J. Struct. Geol.* **3**, 51–65.

Faure, M. & Bonneau, M. 1988. Données nouvelles sur l'extension néogène de l'Egée: La déformation ductile du granite miocène de Mykonos (Cyclades, Grèce). *C.r. Acad. Sci., Paris, Series II* **307**, 1553–1559.

Faure, M., Bonneau, M. & Pons, J. 1991. Ductile deformation and syntectonic granite emplacement during the late Miocene extension of the Aegean (Greece). *Bull. geol. Soc. Fr.* **162**, 3–11.

Fitch, T. J. 1972. Plate convergence, transcurrent faults and internal deformation adjacent to southeast Asia and the western Pacific. *J. geophys. Res.* **77**, 4432–4460.

Fytikas, M., Innocenti, F., Manetti, P., Mazzuoli, R., Peccerillo, A. & Villari, L. 1984. Tertiary to Quaternary evolution of volcanism in the Aegean region. *Spec. Publs geol. Soc. Lond.* **17**, 687–699.

Harding, T. P. & Lowell, J. D. 1979. Structural styles, their plate tectonic habitats and hydrocarbon traps. In: *Petroleum Provinces. Bull Am. Ass. Petrol. Geol.* **63**, 1016–1058.

Henjes-Kunst, F. & Kreuzer, H. 1982. Isotopic dating of pre-Alpidic rocks from the island of Ios (Cyclades, Greece). *Contr. Miner. Petrol.* **80**, 245–253.

Henjes-Kunst, F., Altherr, R., Kreuzer, H. and Hansen, B. T. 1988. Disturbed U–Th–Pb systemics of young zircons and uranothorites: The case of the Miocene Aegean granitoids, Greece. *Chemic. Geol.* **73**, 125–145.

Hsü, K. J. 1991. Exhumation of high-pressure metamorphic rocks. *Geology* **19**, 107–110.

Hutton, D. H. W. 1988. Granite emplacement mechanisms and tectonic controls: inferences from deformation studies. *R. Soc. of Edinburgh Trans. Earth Sci.* **79**, 245–255.

Hutton, D. H. W. & Reavy, R. J. 1992. Strike-slip tectonics and granite petrogenesis. *Tectonics* **11**, 960–967.

Institute of Geological and Mineral Exploration 1983. Geological Map of Greece 1:500000. Inst. Geol. Miner. Explor., Athens.

Jacobshagen, V., Dürr, S., Kockel, F., Kopp, K. O. & Kowalczyk, G., with contributions of Berckhemer, H. & Büttner, D. 1978. Structure and Geodynamic Evolution of the Aegean region. In: *Alps, Apennines, Hellenides* (edited by Cloos, H., Roeder, D. & Schmidt, K.). Schweizerbart, Stuttgart, 537–564.

Jansen, J. B. H. 1973. The geology of Greece, Island of Naxos. Inst. Geol. Miner. Explor., Athens.

Jansen, J. B. H. & Schuiling, R. D. 1976. Metamorphism on Naxos. Petrology and thermal gradients. *Am. J. Sci.* **276**, 1225–1253.

Jones, G. & Robertson, A. H. F. 1991. Tectonostratigraphy and evolution of the Mesozoic Pindos ophiolite and related units, northwestern Greece. *J. geol. Soc. Lond.* **148**, 267–288.

Kreuzer, H., Harre, W., Lenz, H., Wendt, I., Henjes-Kunst, F. & Okrusch, M. 1978. K/Ar-und Rb/Sr- Daten von Mineralen aus dem polymetamorphen Kristallin der Kykladeninsel Ios (Griechenland). *Fortschr. Mineral.* **56**, 69–70.

Ktenas, C. A. 1969. La géologie de l'île de Nikaria (ed. Marinos posthum). *Geol. Geophys. Res.* **13**, 58–86.

Leake, B. E. 1990. Granite magmas: their sources, initiation and consequences of emplacement. *J. geol. Soc. Lond.* **147**, 579–589.

Lee, J. & Lister, G. S. 1992. Late Miocene ductile extension and detachment faulting, Mykonos, Greece. *Geology* **20**, 121–124.

LePichon, X. & Angelier, J. 1979. The Hellenic Arc and Trench system: a key to the neotectonic evolution of the eastern Mediterranean area. *Tectonophysics* **69**, 1–42.

Lister, G. S. & Davies, G. A. 1989. The origin of metamorphic core complexes and detachment faults formed during Tertiary continental extension in the northern Colorado River region, U.S.A. *J. Struct. Geol.* **11**, 65–94.

Lister, G. S., Banga, G. & Feenstra, A. 1984. Metamorphic core complexes of Cordilleran type in the Cyclades, Aegean Sea, Greece. *Geology* **12**, 221–225.

Marakis, G. 1970. Remarks on the age of sulfide mineralization in the Cyclades area. *Ann. geol. Pays Hellen.* **19**, 695–700.

Marinos, G. & Petraschek, W. E. 1956. Laurium. *Geol. Geophys. Res.* **4**, 1–247.

Meissner, B. 1976. Das Neogen von Ost-Samos, Sedimentationsgeschichte und Korrelation. *N. Jb. Geol. Palaönt.* **152**(2), 161–176.

Melidonis, N. G. 1980. The geological structure and mineral deposits of Tinos island (Cyclades-Greece). Inst. Geol. Miner. Expl., Athens.

Okrusch, M. & Bröcker, M. 1990. Eclogites associated with high-grade blueschist in the Cyclades archipelago, Greece: A review. *Eur. J. Mineral.* **2**, 451–478.

Okrusch, M., Seidel, E. & Davis, E. N. 1978. The assemblage jadeite-quartz in the glaucophane rocks of Sifnos (Cyclades, Greece). *Neues Jb. Miner. Abh.* **132**, 284–308.

Oncken, O. 1988. Aspects of the reconstruction of the stress history of a fold and thrust belt (Rhenish Massif, Federal Republic of Germany). *Tectonophysics* **152**, 19–40.

Papanikolaou, D., Sakellariou, D. & Leventis, A. 1991. Microstructural observations on the granite of Ikaria island, Aegean Sea. *Bull. geol. Soc. Greece* **25**, 421–437.

Paterson, S. R., Vernon, R. H. & Tobisch, O. T. 1989. A review of criteria for the identification of magmatic and tectonic foliations in granitoids. *J. Struct. Geol.* **11**, 349–363.

Patzak, M. 1988. Der Amphibolit-Gneis-Körper von Akrotiri, Insel Tinos (Griechenland). Diploma Thesis, Universität Würzburg.

Pe-Piper, G. & Piper, D. J. W. 1989. Spatial and temporal variation in Late Cenozoic back-arc volcanic rocks, Aegean sea region. *Tectonophysics* **169**, 113–134.

Platt, J. P. 1986. Dynamics of orogenic wedges and the uplift of high-pressure metamorphic rocks. *Bull. geol. Soc. Am.* **97**, 1037–1053.

Ramsay, J. G. & Huber, M. I. 1983. *The Techniques of Modern Structural Geology. Vol 1. Strain Analysis.* Academic Press, New York.

Ratschbacher, L., Frisch, W. & Linzer, H. G. 1991. Lateral extrusion in the Eastern Alps, part 2: structural analysis. *Tectonics* **10**, 257–271.

Reinecke, T., Altherr, R., Hartung, B., Hatzipanagiotou, K., Kreuzer, H., Harre, W., Klein, H., Keller, J., Geenen, E. & Böger, H. 1982. Remnants of late Cretaceous high temperature belt on the island of Anafi (Cyclades, Greece). *Neues Jb. Miner. Abh.* **145**, 157–182.

Reutter, K. J., Scheuber, E. & Helmcke, D. 1991. Structural evidence of orogen-parallel strike slip displacements in the Precordillera of northern Chile. *Geol. Rdsch.* **80**, 135–153.

Ridley, J. 1984. Listric normal faulting and the reconstruction of the synmetamorphic structural pile of the Cyclades. In: *The Geological Evolution of the Eastern Mediterranean* (edited by Dixon, J. E. & Robertson, A. H. F.). *Spec. Publs. geol. Soc. Lond.* **17**, 755–762.

Roesler, G. 1978. Relics of non-metamorphic sediments on Central Aegean Islands. In: *Alps, Apennines, Hellenides* (edited by Cloos, H., Roeder, D. & Schmidt, K.). Schweizerbart, Stuttgart, 480–481.

Salemink, J. 1985. On the geology and petrology of Seriphos island, (Cyclades, Greece). *Annl. géol. Pays Hellén.* **33**, 342–365.

Sanderson, D. J. & Marchini, W. R. D. 1984. Transpression. *J. Struct. Geol.* **6**, 449–458.

Schliestedt. M., Altherr, R. & Matthews, A. 1987. Evolution of the Cycladic Crystalline Complex: petrology, isotope geochemistry and geochronology. In: *Chemical Transport and Metasomatism* (edited by Helgeson, H. C. & Schuiling, R. D.). D. Reidel, Dordrecht, 76–94.

Strong, D. F. & Hanmer, S. K. 1981. The leucogranites of southern Brittany: origin by faulting, frictional heating, fluid flux and frictional melting. *Can. Mineralogist* **19**, 163–176.

Sylvester, A. G. 1988. Strike-slip faults. *Bull. geol. Soc. Am.* **100**, 1666–1703.

Tapponnier, P. & Molnar, P. 1977. Active faulting and tectonics of China. *J. Geophys. Res.* **82**, 2945–2969.

Tataris, A. 1964. The Eocene in the semi-metamorphosed basement of Thera island. *Bull. geol. Soc. Greece* **6**, 232–238.

Theodoropoulos, D. 1979. Samos Island, Geological Map 1:50000, with explanations. Inst. Geol. Miner. Expl., Athens.

Van Couvering, J. A. & Miller, J. A. 1971. Late Miocene marine scale and non-marine time scale in Europe. *Nature* **230**, 559–563.

Van der Maar, P. A. & Jansen, J. B. H. 1983. The geology of the polymetamorphic complex of Ios, Cyclades, Greece and its significance for the Cycladic Massif. *Geol. Rdsch.* **72**, 283–299.

Vauchez, A. & Nicolas, A. 1991. Mountain building: strike-parallel motion and mantle anisotropy. *Tectonophysics* **185**, 183–201.

Weidmann, M., Solounias, N., Drake, R. E. & Curtis, G. H. 1984. Neogene stratigraphy of the Eastern basin, Samos island, Greece. *Geobios* **17**, 477–490.

Wernicke, B. & Burchfiel, B. C. 1982. Modes of extensional tectonics. *J. Struct. Geol.* **4**, 105–115.

Wijbrans, J. R. & McDougall, I. 1988. Metamorphic evolution of the Attic Cycladic Metamorphic Belt on Naxos (Cyclades, Greece) utilizing ^{40}Ar–^{39}Ar age spectrum measurements. *J. Metamorph. Geol.* **6**, 1–23.

Zoback, M. D. *et al.* 1987. New evidence on the state of stress of the San Andreas fault system. *Science, N.Y.* **238**, 1105–1111.